Cl_2 dissociation on Si(100)-(2×1): A statistical study by scanning tunneling microscopy

I. Lyubinetsky and Z. Dohnálek
Department of Chemistry, Surface Science Center, University of Pittsburgh, Pittsburgh, Pennsylvania 15260

W. J. Choyke
Department of Physics and Astronomy, University of Pittsburgh, Pittsburgh, Pennsylvania 15260

J. T. Yates, Jr.
Department of Chemistry, Surface Science Center, University of Pittsburgh, Pittsburgh, Pennsylvania 15260

(Received 2 October 1997; revised manuscript received 30 April 1998)

A statistical analysis of the dissociative chemisorption of Cl_2 on the Si(100)-(2×1) surface at 300 K has been carried out in the Cl coverage range up to 0.17 ML using scanning tunneling microscopy. The adsorption of two Cl atoms on Si dimer sites in adjacent silicon dimer rows was found to be kinetically favored (probability P is 0.52). Cl_2 dissociation also occurs with Cl atoms bonded to neighboring Si dimers in the same dimer rows ($P=0.33$). Cl_2 dissociation on a single Si dimer is least likely ($P=0.15$). The least probable Cl pair configuration on a single Si dimer at room temperature is most favored thermodynamically, indicating that kinetic factors control the site selection process at 300 K. The observed selectivity of the Cl pair configurations, produced at 300 K, is consistent with Cl_2 dissociative chemisorption occurring through a mobile precursor-mediated channel. At increasing Cl_2 exposure, the density of the fully Cl-terminated dimers increases, and at saturation the surface consists of only these chlorine configurations. Tunneling spectroscopy has been employed to characterize the Cl-saturated Si(100) surface, and it has been found that filled-state images mainly probe the bonding σ_d states of the Si-Si dimers. Empty-state images probe the antibonding $\sigma^*_{Si\text{-}Cl}$ states in the overlayer. [S0163-1829(98)09735-5]

I. INTRODUCTION

The interaction of Cl_2 with silicon surfaces is of considerable technological importance in the context of dry etching and surface photocleaning. The chemisorption of Cl_2 has been studied previously by a variety of surface analysis techniques (Ref. 1, and references therein). For most molecular adsorbate-surface systems, chemisorption occurs either through a precursor-mediated or a direct mechanism.[2] Recently, a third chemisorption mechanism involving abstraction has been emphasized for the interactions of halogen molecules with silicon surfaces, in particular, for the Cl_2-Si(111) system.[3,4] Fundamental information about Cl_2 adsorption on Si(100) may be obtained using the scanning tunneling microscope (STM). The STM has the unique capability of studying specific sites for chlorine chemisorption with atomic resolution. The STM has been used previously to study site selectivity upon chemisorption of different species only on the Si(111)-(7×7) surface, whose unit cell has a great diversity of active sites.[4–7]

Chlorine adsorption on Si(100) at low coverages was studied using the STM by Boland.[8] Two possible bonding sites were suggested. The first adsorption site involves a Cl atom bonded on the dangling bond of the Si dimer, while the second site is a bridge-bonded Cl atom which is bonded to the two Si atoms of the dimer, and this is a metastable bonding site.[1] Moreover, it was possible to induce transformations between different types of Cl sites by applying an appropriate voltage between tip and sample.[8] At high exposures, Cl forms a (2×1)-ordered structure, which has also been observed in STM studies of the interaction of methyl chloride with the Si(100) surface.[9]

In our previous studies, we showed that the desorption of chlorine atoms from the Cl-saturated Si(100) surface can be achieved underneath the STM tip.[10] In this work, we investigate with the STM the adsorption of chlorine on Si(100)-(2×1) and the formation of the Cl-terminated surface at room temperature. We demonstrate that adsorption site selectivity exists in the initial stages of the Cl_2 chemisorption, which is consistent with the presence of a mobile precursor state. At increasing Cl_2 exposure, the isolated adsorption sites coalesce producing close-packed configurations of the Cl-terminated dimers, which form the saturation surface. The changes of electronic structure induced by Cl adsorption are analyzed on the basis of a simple molecular-orbital approach.

II. EXPERIMENT

All experiments were conducted in an ultrahigh-vacuum (UHV) system equipped with a STM (Omicron), a cylindrical mirror Auger electron analyzer (Physical Electronics Industries), a quadrupole mass spectrometer (UTI Instruments), an ion-sputtering gun and a load-lock system. The base pressure of the system was 6×10^{-11} Torr. The measurements were carried out on the (100) surface of a Si crystal (Virginia Semiconductor, p-type, B-doped, 100 Ω cm). The samples were rinsed in ethanol and deionized water prior to installation into the chamber. There they were degassed at ~900 K for 1 h and flashed several times to 1490 K for ~5 s to produce the atomically clean, well-ordered surface. To avoid

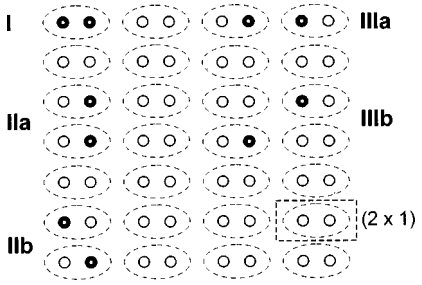

FIG. 1. Schematic of the five geometrically distinguishable configurations of the neighboring pairs of Cl atoms on the Si(100)-(2×1) surface. The Si dimers and the 2×1 unit cell are outlined by dashed lines.

sample contamination, no materials other than tantalum were allowed near the sample.[11] Chlorine gas (Matheson, >99.5%) was purified by freeze-pump-thaw cycles before use. The Cl_2 was introduced into the chamber using an internal pin-hole-type doser,[12] terminated with a stainless-steel tube that releases gas ~4.5 cm away from the STM tunneling junction. To overcome the tip shadow effect, the tip was withdrawn ~400 nm away from the sample surface during Cl_2 exposures. The chlorine coverage was obtained by counting the number of filled adsorption sites from STM images, taking into the account the initial level of defects. All experiments were carried out at room temperature. Sequences of images showing the same region with increasing Cl coverage were acquired. Analysis of the same sample area during progressive adsorption allowed us to identify the initial defects and to monitor changes on the surface caused by the adsorption of single Cl_2 molecules. All STM images shown in this paper are constant current (0.05 nA) topographs.

STM tips were made from electrochemically etched tungsten wire. The tips were cleaned and sharpened *in situ* by several cycles of annealing and Ar^+ bombardment, using the self-sputtering process in the field emission mode.[13] As prepared, the tungsten tips usually had poor long-time stability which is important in the step-by-step study of the Cl_2 adsorption. For that reason, silicon nanotip formation on the tip apex was adopted as a final step of the tip preparation,[14] which was carried out on the Si(100) surface outside the region being studied.

III. RESULTS

A. Initial stages of Cl_2 adsorption on Si(100)

Assuming that dissociative chemisorption of the Cl_2 molecule takes place only on neighboring Si surface atoms, for pairs for Cl atoms there can be only five symmetrically distinctive configurations produced, which involve the Si-atom pairs of Si(100)-(2×1). This is schematically shown in Fig. 1. Depending on the number of Si-Si dimers and the number of dimer rows involved, we distinguish the following three groups: (I) single Si dimer involved, (II) two Si dimers of the same dimer row involved; and (III) two Si dimers of neighboring dimer rows involved. The labels a and b within the groups mark the configurations with linear and diagonal arrangements of two Cl atoms, respectively. The number of equivalent configuration per unit cell, or statistical weight, is 1 for configurations I and IIIa, and 2 for configurations IIa, IIb, and IIIb.

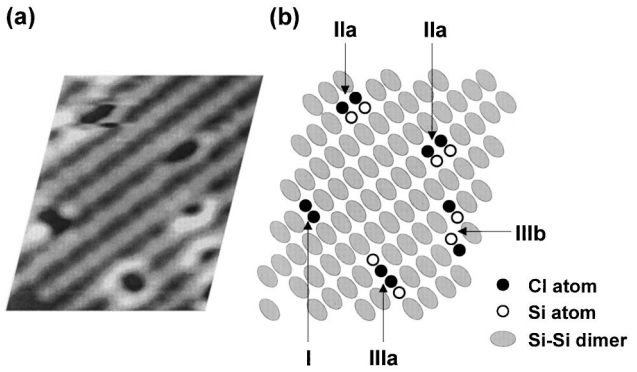

FIG. 2. Image of 46×55-Å^2 region of the Si(100) surface at initial stages of Cl_2 adsorption showing the different Cl adsorption sites. (a) Filled-state STM image at a sample bias of −1.5 V and a tunneling current of 0.05 nA. (b) Schematic identification of the observed features.

We found that Cl-derived features were always paired on the same or adjacent dimers, and isolated Cl atoms were not observed. Figure 2(a) shows the characteristic appearance of the different Cl adsorption sites in the filled-state STM images. The Si dimer rows run diagonally from the bottom left to the top right corners of the image. The dark feature in the left bottom corner is a dimer vacancy defect which existed prior to Cl_2 adsorption. The identification of the configurations of the Cl atoms terminally bound to the Si atoms is schematically represented in Fig. 2(b). The dark dimer unit corresponds to configuration I, where both Si atoms of the same dimer are bonded to Cl atoms.[8,9] All other configurations appear when a single dangling bond of the Si dimer reacts with a Cl atom producing a darkened atom image. The paired features on adjacent dimers of the same or neighboring rows are attributed to the configuration groups II and III, respectively. Each such feature contains the dark and bright counterparts which are localized on opposite sides of the same dimer. The dark Cl-related features appear to be more localized than bright features associated with unoccupied Si single dangling bonds. These bright features have an arclike shape. We observed that switching occurs for Cl atoms from one dimer side to another.[8] Therefore, for the group-II and -III sites, the Cl atoms could be found on either end of the dimers creating several possible configurations. Since we did not observe Cl atoms switching out of an individual silicon dimer, we still can use our classification in the cases where Cl atoms are not close to each other, as, for example, for feature IIIb in the Fig. 2. Probably also due to site switching, we did not clearly observe the IIb configurations.

Figure 3 shows the evolution of the Si(100) surface at initial stages of Cl_2 adsorption. Sequential images of the same surface region at a Cl coverage $\theta = 0$, 0.05, 0.1, and 0.15 ML are presented in Figs. 3(a)–3(d). Figure 3(e) schematically illustrates the configuration changes labeled $A1 \rightarrow A2$ and $B1 \rightarrow B2 \rightarrow B3$. The clean surface shows a well-ordered 2×1 reconstruction with a double missing dimer defect at the top central part of the images. Chlorine exposure leads to the appearance of the paired adsorption sites of different configurations, as outlined previously in Figs. 1 and 2, which are randomly distributed across the surface. Reinspection of the same features with the STM reveals that some of the Cl atoms switch between the two ends of the Si dimer,

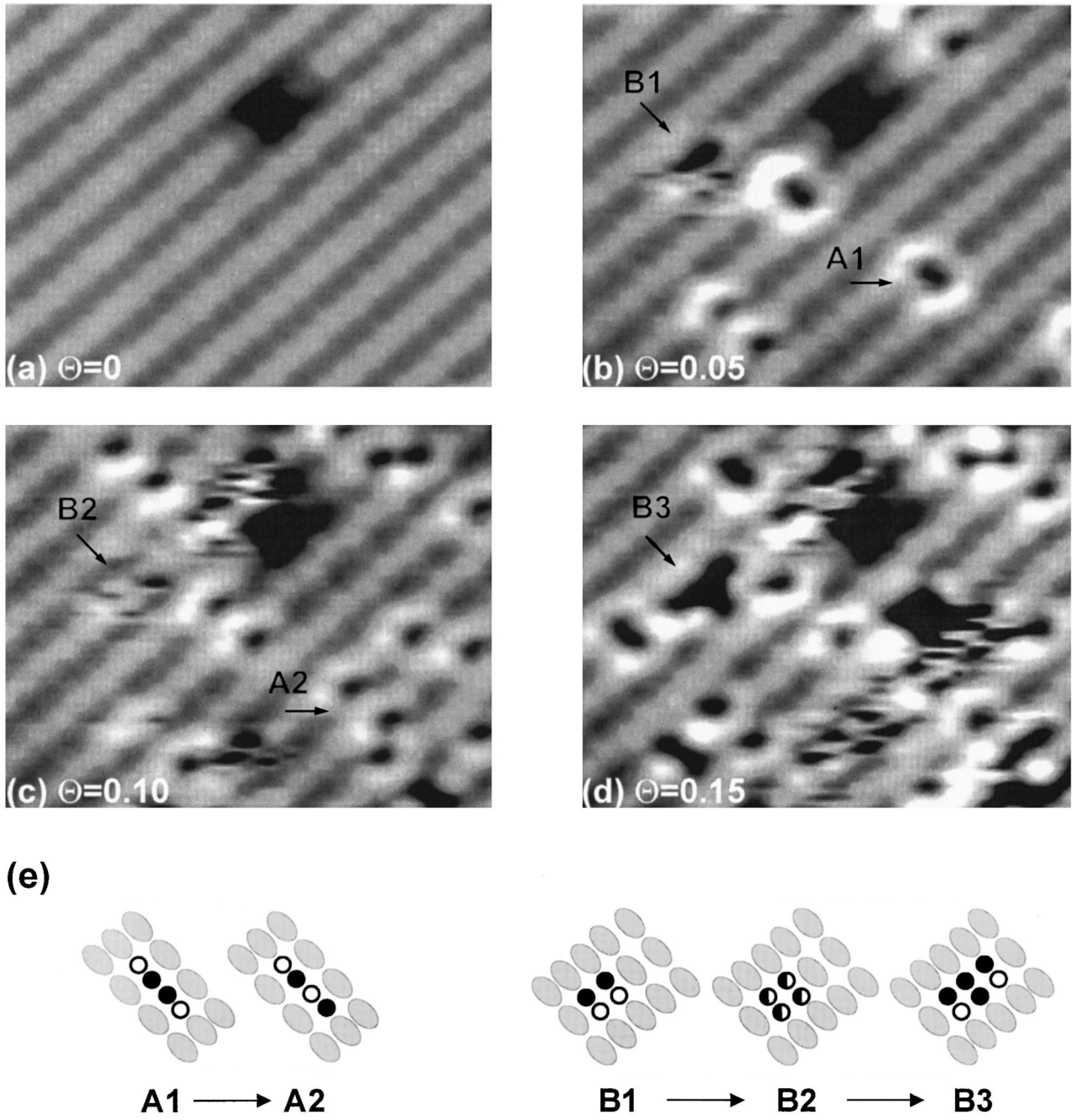

FIG. 3. Evolution of the Si(100)-(2×1) surface at initial stages of Cl adsorption. (a)–(d) Filled-state images (at a sample bias of −1.5 V and a tunneling current of 0.05 nA) of the 42×50-Å^2 region at $\Theta = 0$, 0.05, 0.1, and 0.15 ML, respectively. (e) Schematic illustration of Cl site behavior upon increasing coverage for a process labeled *A* and a process labeled *B* involving various configurations.

as was also observed by Boland.[8] An example of the Cl atom switching is shown in Figs. 3(b) and 3(c), where the configuration IIIa before and after switching is marked as A1 and A2, respectively. Event B1→ B2 represents configuration IIa becoming fuzzy as result of continuous switching of the Cl atom.[8] Evidence of a fuzzy IIa feature appearance (alongside a sharp IIa feature) is also shown in the upper left corner of Fig. 2(a). It was suggested in Ref. 6 that the tip-adsorbate interaction is responsible for this behavior. Chlorine-atom motion to *adjacent* silicon dimers has never been observed using the STM tunneling parameters employed here. At increasing Cl coverage, the isolated configurations start to coalesce producing the most close-packed type-I configuration. This is illustrated by event B2→ B3 in Figs. 3(c) and 3(d), where the adsorption of a Cl_2 molecule at a configuration II produces a dark T-shaped feature as two Cl atoms are added to the type-II site.

B. Statistical distribution of adsorption configurations

By counting the reacted sites in the images, one can determine the relative probabilities for Cl_2 absorption into the different configurations. This can be done only at the initial stages of adsorption when the configurations are isolated from each other and, thus, are distinguishable. We have analyzed ~2100 dimer sites at six Cl coverages, up to θ

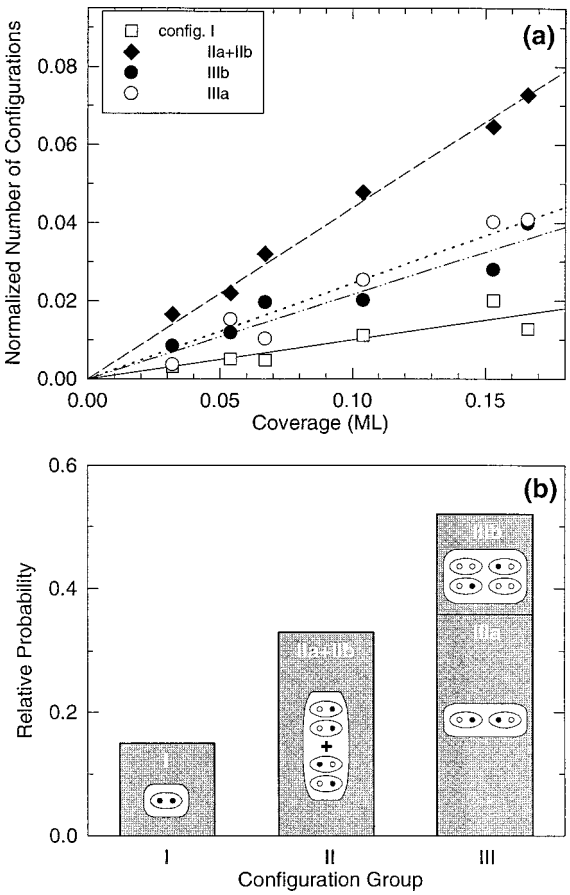

FIG. 4. The population of geometrically distinctive configurations for Cl atom pairs on the Si(100)-(2×1) surface. (a) Normalized number of each type of configuration vs Cl coverage. (b) Relative probabilities of each configuration.

$=0.17$ ML. The number of each type of configuration, normalized to the total number of reacted sites at each coverage, is shown in Fig. 4(a) as a function of the Cl coverage. Due to site switching, configurations IIa and IIb are represented together by their sum. The slope of each curve is proportional to the probability of formation of each configuration, and to within experimental error, the probability of each configuration is independent of coverage, giving linear curves up to $\theta=0.17$ ML. The relative probability for Cl_2 adsorption into each configuration has been obtained by normalization for the statistical weight of each type of configuration and is shown in Fig. 4(b). The normalization for statistical weight Z for the IIa+IIb configurations can be made using the fact that $Z_a=Z_b=2$,

$$P_{\mathrm{IIa+IIb}}=\frac{N_a}{Z_a}+\frac{N_b}{Z_b}=\frac{N_a+N_b}{2}, \tag{1}$$

where $P_{\mathrm{IIa+IIb}}$ is the total probability for configurations IIa and IIb, N_a and N_b are the normalized numbers of each configuration, and Z_a and Z_b are the statistical weights of configurations IIa and IIb. The adsorption probabilities derived from this statistical analysis are given in Table I. The errors in these measurements are statistical rather than being due to uncertainty in the identify of the configurations observed.

TABLE I. Cl_2 adsorption configuration probabilities on Si(100)-(2×1) at 300 K.

Configuration	Probability of formation
I	0.15 ± 0.04
IIa+IIb	0.33 ± 0.03
IIIa	0.36 ± 0.04
IIIb	0.16 ± 0.03

C. Formation of the Cl monolayer

Higher Cl_2 exposures leading to $\theta>0.17$ causes an increase of the density of the type-I configuration of Cl-terminated dimers. Figure 5 shows filled- and empty-state images of the same region of the Si(100) surface before and after Cl saturation. Higher exposure to Cl_2 beyond saturation does not induce further changes indicating complete saturation of the Si dimer dangling bonds. From Fig. 5 one can see that the 2×1 reconstruction is preserved and two atomiclike protrusions, especially in empty-state images, are visible inside the dimers. We usually observed higher resolution on the Cl-saturated surface compared with the clean Si(100) surface, as was also reported for H- (Ref. 15) and Br-saturated Si(100) surfaces.[16] From a comparison of the defect positions on the saturated surface, Figs. 5(c) and 5(d), one can see that the row features in the empty-state images are shifted laterally relative to filled-state images. This differs from filled- and empty-state images of the clean Si(100) surface, Figs. 5(a) and 5(b), where the dimer row features correspond spatially to each other. Figure 6 shows the height profiles, measured along lines AA' and BB' in Figs. 5(c) and 5(d). The profiles reveal that the distance between atomic protrusions is different in the filled- and empty-state images of the Cl-saturated surface (approximately 2.1 and 4.6 Å, respectively).

Three types of defects can be distinguished on the surface before and after saturation. All of them exhibit similar features in the filled- and empty-state images. First, there are initial defects of the clean surface that disappear after the Cl adsorption, as marked by black arrows in Figs. 5(a) and 5(b). These features are probably adsorbates produced from residual gas rather than structural defects. Second, there are initial defects, which are observed even after full coverage of Cl. The defect in top left part of the Fig. 5(a) and 5(b) images is a dimer vacancy which becomes bright after Cl adsorption. It could originate from bridge-bonded Cl at the Si defect site.[17] Third, there are new defects, which appear upon adsorption, as marked by white arrows in Figs. 5(c) and 5(d). These features resemble single-atom vacancies, and are not correlated with initial defect sites.

Laterally averaged tunneling spectra of the clean and Cl-saturated Si(100) surfaces are presented in Fig. 7, which shows the dependence of the logarithm of the absolute value of tunneling current on the sample-bias voltage. It may be seen that the energy gap between the onset voltages for electron tunneling in two directions increases from ~0.9 eV for the clean surface, up to ~1.8 eV for the Cl-saturated surface.

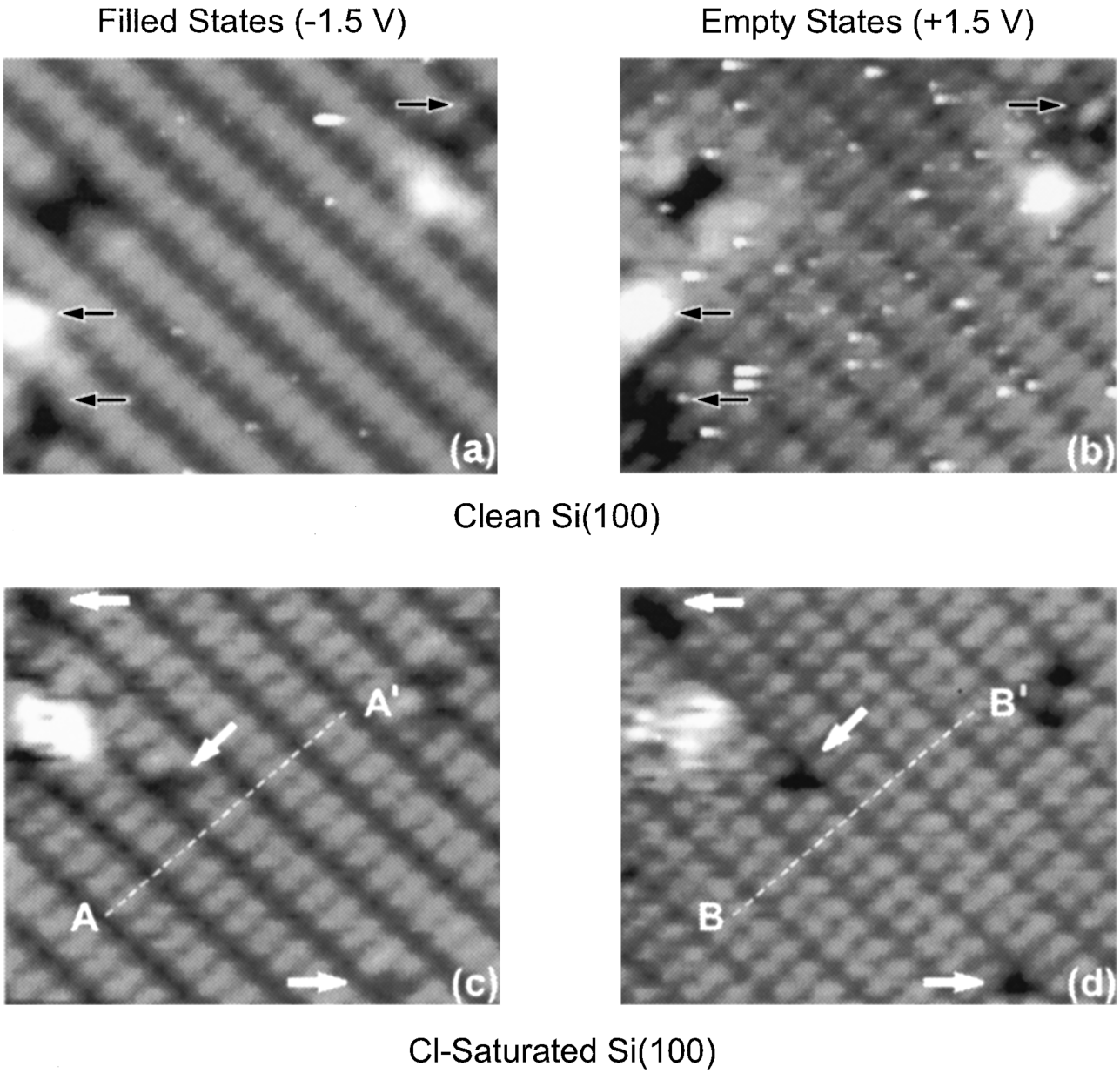

FIG. 5. (a) and (b) Filled (-1.5 V) and empty- ($+1.5$ V) state images of the 39×35-Å^2 region of the Si(100) surface before Cl_2 adsorption. (c) and (d) After Cl saturation. Initial defects in images (a) and (b) which disappear on Cl_2 adsorption and new defects in images (c) and (d) which appear upon adsorption, are marked by black and white arrows, respectively.

IV. DISCUSSION

A. Adsorption configuration selectivity

These experiments clearly show that chlorine adsorption produces Si-Cl terminal bonds at site positions which are systematically correlated on the Si(100) surface. At low coverages, two Cl atoms from a dissociated Cl_2 molecule are always found on neighboring dimer sites of various configurations or on a single silicon dimer. The most probably Cl-Cl configuration is of type III, where adsorption on dimer sites in adjacent dimer rows occurs. The probability for Cl_2 adsorption on nearest-neighboring Si sites in adjacent dimers (IIIa) is $0.36/0.16=2.3$ times higher than on offset adjacent dimers (IIIb) which possess a longer Si-Si separation distance. Less probable Cl-Cl configurations occur within the Si dimer rows (types I and II), with the type-II adsorption being $0.33/0.15=2.2$ times more probable then type-I configuration. The observation of a random distribution of the Cl-atom pairs over the surface at room temperature, and the lack of observation of single Cl atoms, show that chemisorbed Cl is immobile at this temperature. This is consistent with a Cl-Si bond strength of 4.14 eV (Ref. 18) and an activation energy for surface migration of about 1.0 eV.[19] Therefore, the observed adsorption patterns are not caused by Cl diffusion in the chemisorbed state.

We suggest that the site configuration selection process has its origin in the distinctive mechanism of Cl_2 dissociative chemisorption on Si(100)-(2×1). Molecular-beam experiments indicate that at low translational energies the Cl_2 molecule adsorbs on Si(100) at room temperature dominantly via a precursor-mediated mechanism, and that there is a second direct activated chemisorption channel with an activation energy of 0.055 eV.[20] The statistically measured preference (Fig. 4) for dissociative Cl_2 adsorption on silicon dimer sites

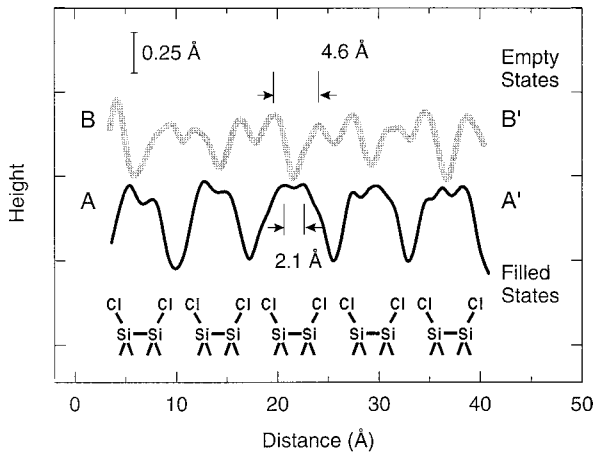

FIG. 6. STM height profiles over filled- and empty-state images for saturated Cl/Si(100). The profiles are measured along lines AA' and BB' in Fig. 5.

which are adjacent to each other in neighboring dimer rows (configuration III) indicates that the activation barrier to chemisorption is minimal for Cl_2 dissociating from a precursor state located between dimer rows. The calculations of the potential-energy surface for a number of diatomic molecule-substrate systems generally show a strong dependence of activation barrier for dissociation on the adsorption site geometry,[21] but, as far as we know, such calculations have not been carried out for the Cl/Si(100) system.

Adsorption of a Cl_2 molecule does not disrupt the silica dimer but breaks the weak surface stabilizing π bond which exists on the clean Si(100)-(2×1) surface.[22] Therefore, for two Cl atoms, double occupation of a dimer would be energetically preferred over the adsorption on two dimers, since one π bond is eliminated instead of two. Indeed, the calculations in Ref. 23 demonstrated [for the H/Si(100) system] that the energy of the type-I configuration is less than that of type-II configuration. The thermodynamic preference for the Cl atoms to form configuration I is also confirmed by STM studies of the Cl-Si(100) system at submonolayer coverages

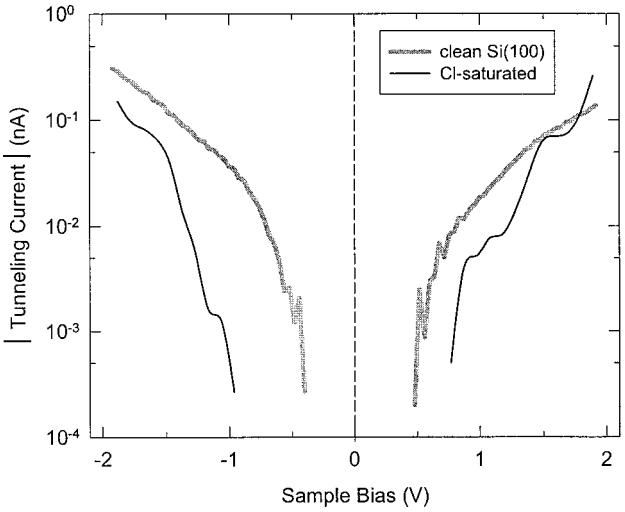

FIG. 7. Laterally averaged tunneling spectra of the clean and Cl-saturated Si(100) surfaces obtained at a reference tunneling current of 0.1 nA and a sample-bias voltage of +1.5 V.

after annealing at >700 K, where only configurations of Cl-saturated silicon dimers have been observed.[24] *Thus the adsorption of Cl_2 at room temperature is controlled by kinetic rather than thermodynamic factors.*

Several factors may influence the activation energy barrier for Cl_2 dissociative adsorption. One of these is the favorable overlap of Si surface-atom orbitals and Cl_2 molecular orbitals. According to calculations for the Si(100)-(2×1) surface,[22,25] there is in fact substantial electron density that localizes near a Si surface atom (for either buckled or symmetric dimers). For a symmetric dimer, while the bonding π states have an electron density maximum between two Si atoms, their electron density contour is located mainly below the surface. This is in contrast to the contours associated with the states localized near Si atoms (and related to the dangling bonds). Since the latter electron-density contours protrude from the surface, their overlap with Cl_2 p_z orbitals has to be taken into consideration. Taking into account that projections of these contours are inclined off the ends of the Si dimers, overlap of Si and Cl_2 orbitals leading to Cl_2 dissociation is favored for type-III configurations, with type IIIa favored over type IIIb. Less favorable overlap of Si dangling bonds occurs for type-II configurations, and the least favorable overlap occurs for type-I configurations.

It is interesting to note that at low coverages different configurations are ''preferred'' by different halogen atoms. There is no simple explanation for the fact that only configurations I and IIa were observed for I/Si(100),[26] and only configuration I was observed for Br/Si(100).[16] Further detailed theoretical studies of the halogen molecule adsorption on the Si(100)-(2×1) surface must be carried out to understand these observed differences.

Because our data do not show the presence of isolated single chemisorbed Cl atoms, the possibility of both abstractive and ''long-range'' dissociative chemisorption of Cl_2 on Si(100) surface can be excluded. In contrast, the abstractive channel does exist for Cl_2 adsorption on the Si(111)-(7×7) surface.[4] We attribute this difference to the very different dangling-bond character of these silicon surfaces. As a result, in contrast to the Si(100) surface, the primary mechanism for adsorption of Cl_2 on Si(111) is directly activated chemisorption/abstraction, while a precursor-mediated channel is minor.[4,20]

B. Electronic structure changes upon Cl adsorption

Cl adsorption induces changes in electronic structure which are exhibited in the tunneling spectra and are responsible for the appearance of the Cl-derived features in the STM images. This can be understood qualitatively with the help of a simple molecular-orbital approach, similar to the one used by Wang, Bronikowski, and Hamers for the H/Si(100) system.[27] Figure 8 shows a schematic energy-level diagram for the Si dimer (a) before and after adsorption of (b) one and (c) two Cl atoms per dimer. On the clean 2×1 dimer-reconstructed Si(100) surface, each Si surface atom has two sigma back bonds (σ_b), a dimer sigma bond (σ_d), and an sp^3-hybridized dangling bond.[22] Dangling bonds interact with each other via weak π bonding, and exhibit a difference between the occupied π_d bonding and unoccupied π_d^* antibonding states of around 1 eV,[22,28,29] as shown in

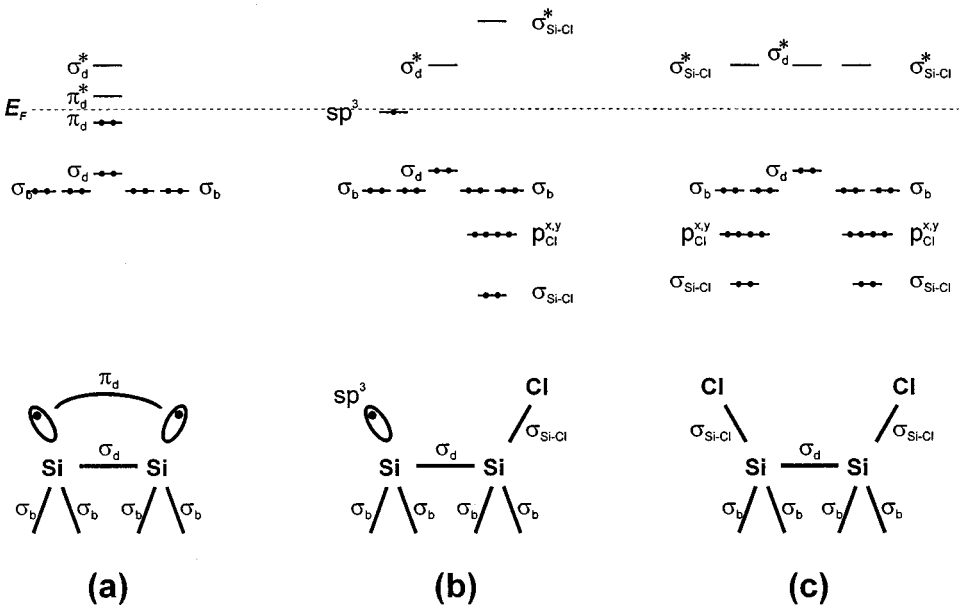

FIG. 8. (a) Schematic energy-level diagram for the Si dimer before Cl_2 adsorption. (b) After adsorption of one Cl atom per Si dimer. (c) After adsorption of two Ci atoms per Si dimer. Some of the energy levels which reside far from Fermi level (e.g., s_{Cl} at ~ -16 eV) (Ref. 18) are not shown for simplicity.

Fig. 8(a). These states, closest to the Fermi level (E_F), mainly determine the STM images of the clean Si(100)-(2 $\times$1) surface for both tunneling bias polarities.[30] Upon the adsorption of a single Cl atom on a Si dimer, the π_d bond is broken and one Si-Cl σ bond is formed by interaction between the Si dangling bond and primarily the Cl p^z orbital.[18,31] This leaves an unpaired sp^3 dangling bond on the second Si atom, as shown in Fig. 8(b). The position of the Cl-derived $\sigma_{Si\text{-}Cl}$ and $\sigma^*_{Si\text{-}Cl}$ states upon adsorption of a single Cl atom on a Si dimer can be estimated from existing calculations for Cl/Si(111).[32] The unpaired sp^3 dangling bond (half-filled) lies near the Fermi level, and therefore appears brighter than ''clean'' Si dimers in the STM images.[9,15] Upon adsorption of a pair of Cl atoms on a Si dimer, Fig. 7(c), two $\sigma_{Si\text{-}Cl}$ bonds are formed. Both *ab initio* calculations[18] and molecular-orbital calculations[31] placed the occupied $\sigma_{Si\text{-}Cl}$ bonding states and Cl $p^{x,y}$ states (mainly nonbonding) at $\sim$7 and $\sim$5 eV below E_F, respectively. Electron-energy-loss spectroscopy experiments[33] have detected an electronic transition between $\sigma_{Si\text{-}Cl}$ bonding and $\sigma^*_{Si\text{-}Cl}$ antibonding states at 8.8 eV, and consequently, the unoccupied $\sigma^*_{Si\text{-}Cl}$ states lie at $\sim$2 eV above E_F. Thus the density of states around the Fermi level is significantly decreased upon Cl adsorption, and Cl-terminated Si atoms therefore appear darker in STM images than unreacted Si atoms.

An energy difference between onset bias voltages of $\sim$0.9 eV in the tunneling spectra of the clean Si(100) (Fig. 7) is the difference between the filled π and empty π^* states, as can be seen in Fig. 8(a). This value agrees well with previous studies of the clean Si(100) surface.[30] After saturation by chlorine, the tunneling spectrum exhibits a much wider gap of $\sim$1.8 V, as shown in Fig. 7. From the energy-level diagram in Fig. 8(c), one can see that at low-bias voltages mainly the filled dimer σ_d bonding states and unfilled $\sigma_{Si\text{-}Cl}$ antibonding states participate in tunneling for filled- and empty-state images, respectively. Despite approximately the same energy position of the dimer unoccupied σ^*_d states and the $\sigma^*_{Si\text{-}Cl}$ antibonding states, the $\sigma^*_{Si\text{-}Cl}$ states are more spatially extended out from the surface due to the Cl-atom projection from the surface and, thus, they are mainly accessible for imaging by the STM. As discussed above, the unoccupied $\sigma^*_{Si\text{-}Cl}$ states lie at $\sim$2 eV above E_F. We suggest that the tunneling current increase at voltages more than $\sim$+0.8 V is due to tunneling into the tail of the $\sigma^*_{Si\text{-}Cl}$ states, which strongly disperses over the Brillouin zone.[34] Conversely, tunneling current at voltages less than ~ -1 V occurs through tunneling into the tail of the occupied dimer σ_d states. The calculations place the σ_d states at above 3 eV below E_F, within a band from -1.5 to -3.5 eV.[28,29] Moreover, a projection of the Si bulk density of states is nonzero in some regions of the surface Brillouin zone,[18,29] and therefore additional broadening of the σ_d states is anticipated because of hybridization within the bulk.

C. Structure of the Cl-saturated Si(100) surface

Our data show that the formation of the saturated Cl layer occurs by dissociation of Cl_2 molecules and the termination of both dangling bonds of the Si dimers. This is the first direct experimental demonstration that a saturated Cl/Si(100) surface exhibits a coverage of one Cl per Si, although other data have also indicated this fact.[1,9] Monolayer formation occurs through the increase of the density and coalescence of the different Cl configurations. This finally leads to a Cl-saturated Si(100) surface consisting only of fully saturated dimers (type-I configuration).

Since the empty-state images of the Cl-saturated Si(100) are formed by the $\sigma^*_{Si\text{-}Cl}$ states, as discussed above, the spatial distribution of these $\sigma^*_{Si\text{-}Cl}$ orbitals are presumably responsible for two-lobed empty-states images shown in Fig. 5(d), and the two lobes correspond to Cl atoms bonded to Si dimer atoms in adjacent rows. The lateral apparent shift of the rows of two-lobed features in going from filled-state im-

ages to empty-state images of the saturated Cl/Si(100) surface (Fig. 6) can be understood by taking into consideration that the Si-Cl bond is inclined $25° \pm 4°$ off normal.[1] This brings the Cl atoms on adjacent silicon dimer rows in close proximity, giving close-packed $\sigma^*_{\text{Si-Cl}}$ state images, and leading to a lateral shift in the row position. On the other hand, filled-state images for the saturated Cl/Si(100) surface are formed primarily by the σ_d orbitals which are controlled by the silicon-atom positions. Hence the filled-state images for saturated Cl/Si(100) correspond approximately in lateral position to the Si-atom structures seen on clean Si(100)-(2 ×1), and no lateral shift of the rows is observed in comparing the filled-state images of Figs. 5(a) and 5(c).

V. CONCLUSIONS

Adsorption of Cl_2 molecules on the Si(100)-(2×1) surface at room temperature has been studied by the STM. Dissociative chemisorption occurs only on nearest-neighboring sites, and chlorine atoms are always observed in pairs. The statistical arrangement observed for Cl-atom pairs at coverages below 0.17 ML indicates that the adsorption of single Cl atoms on Si atoms in adjacent silicon dimer rows is kinetically favored, with a probability of 0.52. Adsorption on neighboring Si dimers in the same dimer row occurs with a probability of 0.33. Adsorption on a single Si dimer is less favorable, with a probability of 0.15. On purely thermodynamic grounds adsorption of two Cl atoms on a single Si dimer site is most favorable. Thus the kinetically controlled configurations produced at room temperature are metastable configurations. The observed selectivity of the Cl pair configurations is consistent with Cl_2 dissociative chemisorption occurring through a mobile precursor-mediated channel. The favorable steric interaction of the Cl_2 molecular orbitals and Si surface-atom orbitals on adjacent dimer rows influences the activation energy barrier for dissociative chemisorption at these sites compared to other double-site configurations.

At increasing Cl_2 exposure, the isolated double adsorption sites start to coalesce, producing configurations in which single Si dimers are bonded to two Cl atoms, forming the Cl-saturated surface. Tunneling spectroscopy measurement on the saturated Cl/Si(100) surface suggest that filled-state STM images mainly sample the Si-Si dimer σ_d orbitals, whereas empty-state images sample the $\sigma^*_{\text{Si-Cl}}$ orbitals in the Cl saturated layer.

ACKNOWLEDGMENT

We thank the Office of Naval Research for supporting this research.

[1] Q. Gao, C. C. Cheng, P. J. Chen, W. J. Choyke, and J. T. Yates, Jr., J. Chem. Phys. **98**, 8308 (1993).
[2] W. H. Weinberg, in *Kinetics of Interface Reactions*, edited by M. Grunze and H. J. Kreuzer (Springer, Berlin, 1987), p. 94.
[3] Y L. Li, D. P. Pullman, J. J. Zhang, M. T. Schulberg, D. J. Gladstone, M. McGonigal, and S. T. Ceyer, Phys. Rev. Lett. **74**, 2603 (1995).
[4] J. A. Jensen, C. Yan, and A. C. Kummel, Phys. Rev. Lett. **76**, 1388 (1996).
[5] R. Wolkow and P. Avouris, Phys. Rev. B **39**, 1049 (1989).
[6] X. H. Chen, Q. Kong, J. C. Polanyi, D. Rogers, and S. So, Surf. Sci. **340**, 224 (1995).
[7] D. Rogers and T. Tiedje, Phys. Rev. B **53**, 13 227 (1996).
[8] J. J. Boland, Science **262**, 1703 (1993).
[9] M. J. Bronikowski and R. J. Hamers, J. Vac. Sci. Technol. A **13**, 777 (1995).
[10] Z. Dohnálek, I. Lyubinetsky, and J. T. Yates, Jr., J. Vac. Sci. Technol. A **15**, 1488 (1997).
[11] H. Nishino, W. Yang, Z. Dohnálek, V. A. Ukraintsev, and J. T. Yates, Jr., J. Vac. Sci. Technol. A **15**, 182 (1997).
[12] M. J. Bozack, L. Muehlhoff, J. N. Russell, Jr., W. J. Choyke, and J. T. Yates, Jr., J. Vac. Sci. Technol. A **5**, 1 (1987).
[13] A. P. Janssen and J. P. Jones, J. Phys. D **4**, 118 (1971); O. Albrektsen, H. W. M. Salemink, K. A. Mørch, and A. R. Thölen, J. Vac. Sci. Technol. B **12**, 3187 (1994).
[14] R. M. Ostrom, D. M. Tanenbaum, and A. Gallagher, Appl. Phys. Lett. **61**, 925 (1992); S. Heike, T. Hashizume, and Y. Wada, J. Appl. Phys. **80**, 4182 (1996).
[15] J. J. Boland, J. Vac. Sci. Technol. A **10**, 2458 (1992).
[16] D. Rioux, M. Chander, Y. Z. Li, and J. H. Weaver, Phys. Rev. B **49**, 11 071 (1994).
[17] W. Yang, Z. Dohnálek, W. J. Choyke, and J. T. Yates, Jr., Surf. Sci. **392**, 8 (1997).
[18] P. Krüger and J. Pollmann, Phys. Rev. B **47**, 1898 (1993).
[19] G. S. Khoo and C. K. Ong, Phys. Rev. B **52**, 2574 (1995).
[20] D. J. Sullivan, H. C. Flaum, and A. C. Kummel, J. Chem. Phys. **97**, 12 051 (1993).
[21] A. E. De Pristo, in *Dynamics of Gas-Surface Interactions*, edited by C. T. Rettner and M. N. R. Ashfold (The Royal Society of Chemistry, Cambridge, 1991), p. 47.
[22] J. A. Appelbaum, G. A. Baraff, and D. R. Hamann, Phys. Rev. B **14**, 588 (1976).
[23] A. Vittadini, A. Selloni, and M. Casarin, Phys. Rev. B **49**, 11 191 (1994).
[24] Z. Dohnálek, I. Lyubinetsky, and J. T. Yates, Jr. (unpublished).
[25] J. Pollmann, P. Krüger, and A. Mazur, J. Vac. Sci. Technol. B **5**, 945 (1987).
[26] D. Rioux, F. Stepniak, R. J. Pechman, and J. H. Weaver, Phys. Rev. B **51**, 10 981 (1995).
[27] Y. Wang, M. J. Bronikowski, and R. J. Hamers, J. Vac. Sci. Technol. A **12**, 2051 (1994).
[28] G. P. Kerker, S. G. Louie, and M. L. Cohen, Phys. Rev. B **17**, 706 (1978).
[29] S. Ciraci, R. Butz, E. M. Oellig, and H. Wagner, Phys. Rev. B **30**, 711 (1984).
[30] R. J. Hamers, P. Avouris, and F. Bozso, Phys. Rev. Lett. **59**, 2071 (1987).
[31] B. I. Craig and P. V. Smith, Surf. Sci. **290**, L662 (1993).
[32] Self-consistent pseudopotential calculations for Cl-Si(111) (Ref. 34) show that $\sigma^*_{\text{Si-Cl}}$ states are about 4 eV, and disperse in a band from ~2 to ~6 eV above E_F.
[33] N. Aoto, E. Ikawa, and Y. Kurogi, Surf. Sci. **199**, 408 (1988).
[34] M. Schlüter and M. L. Cohen, Phys. Rev. B **17**, 716 (1978).